Table 1 Measured acoustic mode suppressions in a turbofan engine

Configuration	Duct SPL, 60 Hz
Baseline[a]	181 dB
Baseline[b]	161 dB
Helmholtz resonator[a]	163 dB
Helm. res. (tube + 7%)[a]	161 dB
Vanes[a]	162 dB
Vanes[b]	158 dB
Bleed air (4.5% area)[a]	174 dB
Bleed air (5.5% area)[a]	169 dB

[a]Valve closed.
[b]Valve open.

may be treated as single cavity openings having its own associated impingement length.

Two equally spaced vanes were installed in the baseline configuration ducting system opening to nominally triple the ducting system shear-layer frequency (Fig. 1). Shear-layer frequency calculations predict an increase in the primary shear-layer frequency range to 630–1260 Hz. This, in turn, increased the minimum subharmonic shear-layer frequency range to 126–252 Hz. These predicted subcavity opening shear-layer frequency ranges are well outside of the cavity primary acoustic mode frequency range of 55–75 Hz.

With vanes installed in the mouth of the ducting system, and its valve closed, the SPL in the ducting system at 60 Hz was reduced from 181–161.5 dB. With the valve open, the ducting system SPL at 60 Hz was further reduced to 158 dB, and no new acoustic resonances were observed. Similarly, ducting system strain and acceleration levels were reduced by an order of magnitude.

Continuous Bleed Flow

The shear layer can be drawn into the cavity by continually bleeding fluid through the cavity (Fig. 1). Only the minimum required amount of fluid should be allowed through the cavity to minimize the effects on system performance. Minimal flow through the duct may be achieved by drilling holes in the downstream valve's butterfly, or in the cavity wall. (Note that the effectiveness of these holes to draw the shear layer into the cavity is dependent upon their location within the cavity, and their geometry.)

Calculations to determine the minimum flow required to draw the shear layer into the duct are possible. The required ducting system pressure and flow data were not available for this investigation. The minimum flow required to suppress the acoustic mode was established by sequentially increasing the area of a bleed hole in the duct.

Engine test results show that no significant reduction of the ducting system acoustic mode SPL was realized until a hole area equal to 4.5% of the duct area was achieved. The ducting system SPL at 60 Hz was reduced from 181–174 dB for this bleed hole area. When the bleed hole was increased to 5.5%, the SPL was further reduced to 169 dB at 60 Hz. All strain gauges and accelerometers responded consistent with the dynamic pressure transducers.

Conclusions

Full-scale engine test results show that installing a Helmholtz resonator side branch in the cavity, installing vanes in the cavity mouth, and drawing the shear layer into the cavity via continuous minimum bleed flow through the duct, will significantly reduce the SPL of cavity acoustic modes resonantly excited by its shear layer. Table 1 lists full-scale turbofan engine test results that quantify the effectiveness of each method. These results demonstrate that there are several options for extending the structural fatigue life of cavity systems in lieu of potentially expensive structural redesign efforts aimed at increasing the load-bearing capacity of the cavity and its neighboring structures.

Acknowledgments

The author thanks the following employees of Rohr Inc. who contributed to this paper: Robert D. Blevins, Krish Chilukuri, Ian Holehouse, Bill Ingram, Mike Sandlin, Ken Scalapino, and Robert Walters.

References

[1]Rockwell, D., and Knisely, C., "The Organized Nature of Flow Impingement Upon a Corner," *Journal of Fluid Mechanics*, Vol. 93, Pt. 3, 1979, pp. 412–432.

[2]Sarohia, V. "Experimental Investigation of Oscillations in Flow Over Shallow Cavities," *AIAA Journal*, Vol. 15, No. 7, 1977, pp. 984–991.

[3]Ziada, S., and Rockwell, D., "Oscillations of an Unstable Mixing Layer Impinging Upon an Edge," *Journal of Fluid Mechanics*, Vol. 124, June 1982, pp. 307–334.

[4]Knisely, C., and Rockwell, D. "Self-sustained Low-frequency Components in an Impinging Shear Layer," *Journal of Fluid Mechanics*, Vol. 116, June 1981, pp. 157–186.

[5]Blevins, R. D., "Fluid Systems," *Formulas for Natural Frequency and Mode Shape*, Van Nostrand Reinhold, reprinted by Robert E. Krieger, Malabar, FL, 1984, pp. 337–385.

Pitch Rate/Sideslip Effects on Leading-Edge Extension Vortices of an F/A-18 Aircraft Model

Sheshagiri K. Hebbar,* and Max F. Platzer†
Naval Postgraduate School, Monterey, California 93943
and
Odilon V. Cavazos‡
Naval Air Station, San Diego, California 92152

Introduction

THE continuing demands for enhanced maneuverability of present and future fighter aircraft require a better understanding of the vortical flows generated during flight at high angles of attack (AOA). The vortex-bursting phenomenon is of particular importance and has been investigated extensively on stationary wings,[1] but experimental data for wings in unsteady motion are still rather scarce.[2,3] Data for complete aircraft configurations are even scarcer.[4,5] The investigation reported here is a continuation of work done by Hebbar, et al.[6] and focuses on the effect of pitch rate on the development and bursting of vortices generated from the leading-edge extensions (LEXs) of an F/A-18 aircraft model in the 0–50 deg AOA range, at sideslip angles of 0, 5, 10, and 20 deg. Additional details of the experimental investigations appear in Refs. 7 and 8.

Presented as Paper 91-0280 at the AIAA 29th Aerospace Services Meeting, Reno, NV, Jan. 7–10, 1991; received Feb. 4, 1991; revision received July 26, 1991; accepted for publication Sept. 11, 1991.

*Adjunct Professor, Department of Aeronautics and Astronautics. Associate Fellow AIAA.

†Professor, Department of Aeronautics and Astronautics. Associate Fellow AIAA.

‡Lieutenant, United States Navy.

Experiment

Water Tunnel Facility and Aircraft Model

The investigations were conducted in the Naval Postgraduate School (NPS) continuous flow water tunnel. The test section is nominally 38-cm (15-in.) wide, 51-cm (20-in.) high, and 152-cm (60-in.) long. Water velocities of up to 30.5 cm/s (1 ft/s) are possible with a turbulence level of less than 1%. The model support system attached to the top of the test section utilizes a C-strut to vary the pitch angle travel up to 50 deg, and a turntable to provide yaw variations up to ±20 deg (Fig. 1a). The model attitude control system controls two axes (pitch and yaw). The fighter model used was a 1/48th scale model of the McDonnell Douglas Corporation's F/A-18 fighter aircraft (Fig. 1b), with an overall length of 36.2 cm (14.25 in.) and a wing span of 23.8 cm (9.375 in.). The model was equipped with several dye injection ports as shown.

Test Conditions and Vortex Visualization

The experiments were conducted in two phases. The first phase involved the vortex flow visualization on the model for static conditions in the AOA range α = 0–50 deg, at sideslip angles of β = 0, 5, 10, and 20 deg. The second phase involved the dynamic vortex flow visualization on the model for two pitch rates, with angle of attack varying from 0–50 deg (simple pitch-up motion) and 50–0 deg (simple pitch-down motion), both at sideslip angles of 0, 5, 10, and 20 deg. The flow velocity in the water tunnel was nearly constant at 7.5 cm/s (0.25 ft/s), corresponding to a nominal Reynolds number of 76,000/m (23,000/ft). The reduced pitch rates were 0.08 and 0.19. The reduced pitch rate is defined by $\dot{\alpha}L/2U_\infty$ where L is model length, U_∞ is freestream velocity, and $\dot{\alpha}$ is pitch rate in radians/s. The model pitch-axis was located at X/L = 0.505. The observed flow phenomena during static and dynamic conditions were documented with extensive videotape recording and 35-mm photography of the model flowfield in both planview and sideview.

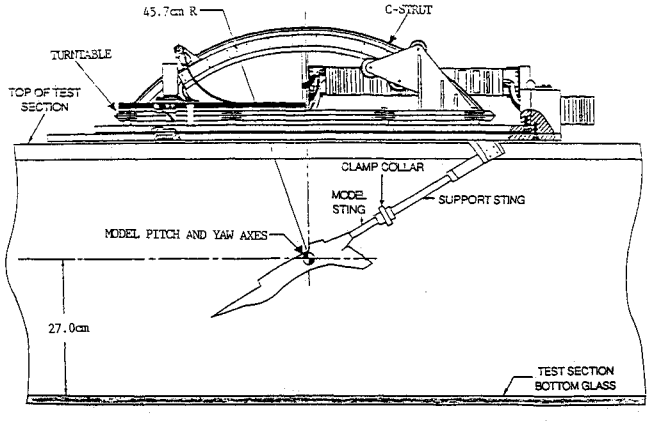

Fig. 1a Model support system of the NPS water tunnel.

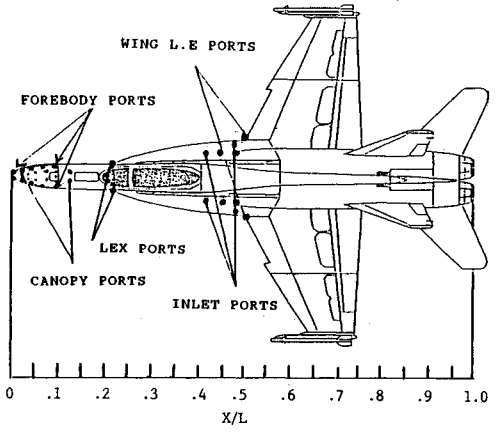

Fig. 1b Two-percent scale model of F/A-18 fighter aircraft with dye-injection ports.

Results and Discussion

Data reduction essentially consisted of measuring the burst location of the vortex shed off the LEX and plotting it as a function of AOA. All measurements were taken on the leeward side of the model using the nose as the reference point. The bursting locations were visually determined from the photographs with the utmost care and consistency, the longitudinal distance X of vortex burst point measured from the nose and scaled for nondimensionalization using the model length L.

Angle-of-Attack Effects on LEX Vortex Core Bursting

Figure 2 presents burst location plots for LEX vortices during pitch-up and pitch-down motion at zero sideslip. Compared with the static curve (also shown in the figure), the burst location during pitch-down motion always occurs earlier. During the pitch-up motion at high AOA (>25 deg), the burst location occurs later relative to the static case. Thus, the burst location curve consistently undershoots the static curve during pitch-down motion, but overshoots during pitch-up motion at high AOA (>25 deg), the undershoot/overshoot increasing with pitch rate. The vortex breakdown response observed here is similar to the one observed by Magness et al.[3] for delta wings. The implications of these overshoots/undershoots during pitch-up and pitch-down motions are noteworthy in that they qualitatively support the increase/decrease in measured lift for pitching motions reported by Brandon and Shah.[4]

Sideslip Effects on Vortex Core Bursting

Figure 3 summarizes the effects of sideslip on burst location of the LEX vortex for the static case. The effect of small sideslip up to 10 deg is to delay bursting for AOA greater

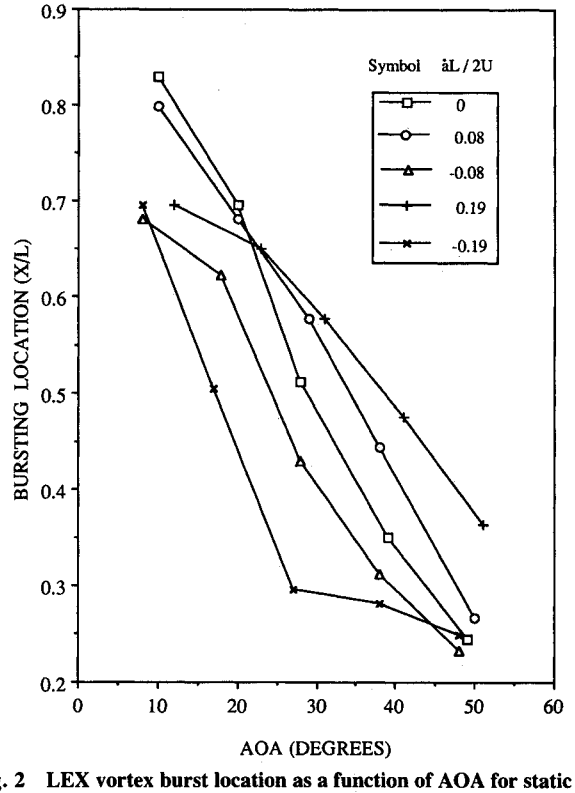

Fig. 2 LEX vortex burst location as a function of AOA for static and dynamic case at zero sideslip angle.

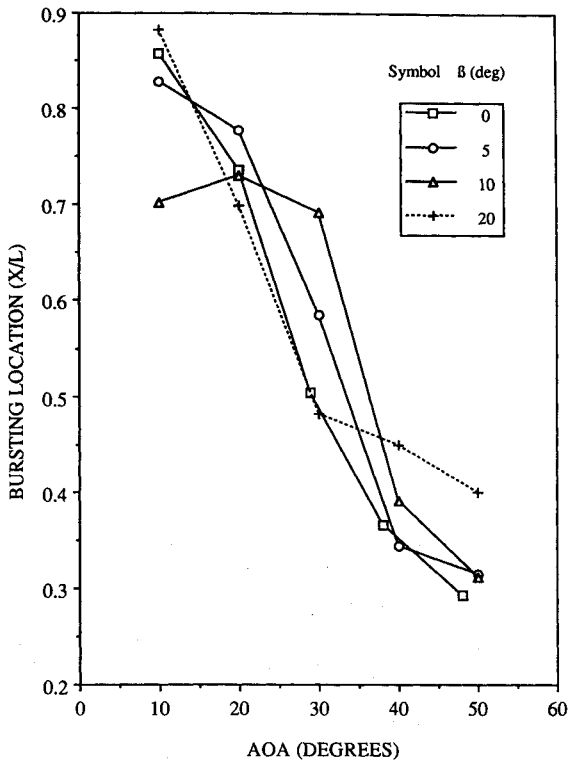

Fig. 3 Leeward side LEX vortex burst location as a function of AOA for static case at different sideslip angles.

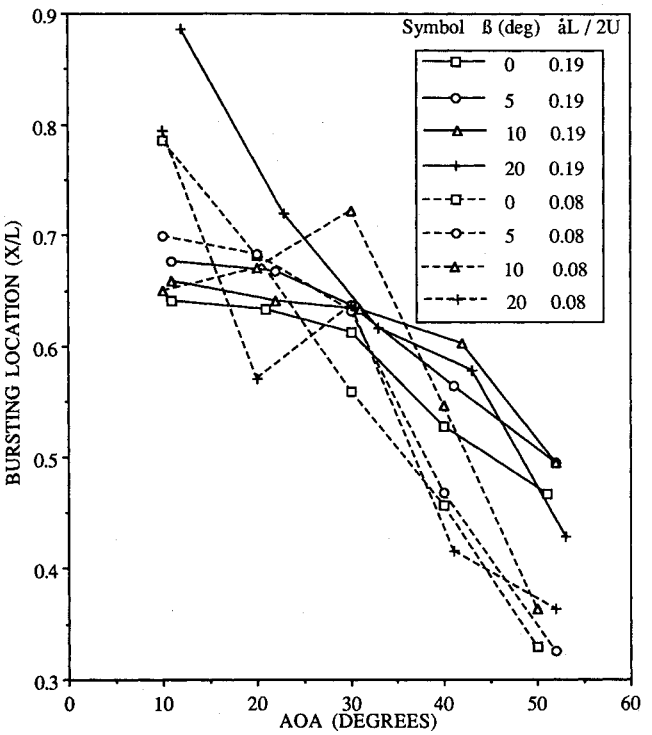

Fig. 4 Leeward side LEX vortex burst location as a function of AOA for two pitch-up motions at different sideslip angles.

than approximately 20 deg. For AOA less than 15 deg, the sideslip causes the dye streak to split, making it difficult to measure the burst location accurately.[7,8] Increasing the sideslip angle to 20 deg causes a large rolling vortex to form at AOA > 20 deg, which increases in size with increasing AOA.

Figure 4 shows burst location plots highlighting the sideslip effect during pitch-up motion at two reduced pitch rates. At the lower pitch rate, the sideslip effects are similar to those observed for the static case. At the higher pitch rate, throughout the range of AOA and sideslip, the bursting is delayed

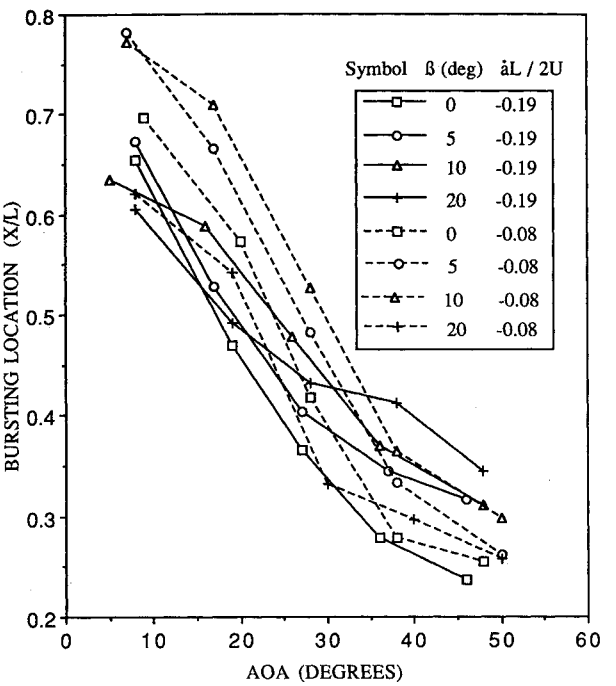

Fig. 5 Leeward side LEX vortex burst location as a function of AOA for two pitch-down motions at different sideslip angles.

relative to the high pitch rate motion at zero sideslip. The two irregular points corresponding to $\alpha = 12$ deg, $\beta = 20$ deg, and $\alpha = 23$ deg, $\beta = 20$ deg, are the result of splitting of the dye streak on the windward side flow and the subsequent merging of the split segment with the leeward vortex.[7,8]

The burst location plots shown in Fig. 5 highlight the sideslip effect during pitch-down motion at two reduced pitch rates. It can be seen clearly that during the lower pitch rate, motion sideslip angles up to 10 deg cause a delay in vortex bursting relative to the corresponding motion at zero sideslip. Increasing the sideslip angle to 20 deg causes a large rolling vortex to develop. At the higher pitch rate, a delay in the vortex bursting is seen for AOA > 11 deg for $\beta = 5$ deg, and 10 deg and for AOA > 16 deg for $\beta = 20$ deg. The undershoot for $\beta = 20$ deg curve (AOA < 16 deg) is due to the splitting of dye streak that results in early bursting.

Conclusions

1) Pitch-rate effects: During the pitch-down motion, the bursting occurs earlier relative to the static case. During the pitch-up motion, the bursting occurs later relative to the static case for AOA > 25 deg. These pitch rate effects increase with pitch rate. 2) Sideslip effects: At a constant AOA, the windward LEX vortex burst location travels forward, inboard, and downward with sideslip, while the leeward LEX vortex burst location travels aft, outboard, and upward. These effects lead to significant vortex asymmetries for both static and dynamic conditions.

Acknowledgment

This work was sponsored by the Naval Air Systems Command and the Naval Postgraduate School. The authors sincerely thank the technical editor for pointing out a plotting error in one of the graphs.

References

[1]Wedemeyer, E., "Vortex Breakdown," *AGARD Lecture Series No. 121, High Angle of Attack Aerodynamics*, Dec. 1982, pp. 9-1 to 9-17.

[2]Lee, M., and Ho, C.-M., "Vortex Dynamics of Delta Wings," *Frontiers in Experimental Fluid Mechanics*, edited by M. Gad-el-Hak, Vol. 46, Lecture Notes in Engineering, Springer-Verlag, Berlin, 1989, pp. 365–428.

[3]Magness, D., Robinson, O., and Rockwell, D., "Control of Leading-Edge Vortices on a Delta Wing," AIAA Paper 89-0999, Tempe, AZ, March 1989.

[4]Brandon, J. M., and Shah, G. H., "Unsteady Aerodynamic Characteristics of a Fighter Model Undergoing Large Amplitude Pitching Motions at High Angles of Attack," AIAA Paper 90-0309, Reno, NV, Jan. 1990.

[5]DelFrate, J. H., and Zuniga, F. A., "In-Flight Flow Field Analysis on the NASA F-18 High Alpha Research Vehicle with Comparisons to Ground Facility Data," AIAA Paper 90-0231, Reno, NV, Jan. 1990. (See also NASA TM 4193, May 1990).

[6]Hebbar, S. K., Platzer, M. F., Park, S. N., and Cavazos, O. V., "A Dynamic Flow Visualization Study of a Two-Percent F/A-18 Fighter Aircraft Model at High Angles of Attack," NASA High-Angle-of-Attack Technology Conference, Oct.–Nov. 1990, Hampton, VA. (Also to appear as NASA CP, 1991.)

[7]Cavazos, O. V., "A Dynamic Flow Visualization Study of LEX-Generated Vortices on a Scale Model of a F/A-18 Fighter Aircraft at High Angles of Attack," Master's Thesis, Naval Postgraduate School, Monterey, CA, June 1990.

[8] Hebbar, S. K., Platzer, M. F., and Cavazos, O. V., "A Water Tunnel Investigation of the Effects of Pitch Rate and Yaw on LEX-Generated Vortices of an F/A-18 Fighter Aircraft Model," AIAA Paper 91-0280, Reno, NV, Jan. 1991.

Thin-Airfoil Correction for Panel Methods

J. Carter* and P. S. Jackson†
University of Auckland, Auckland, New Zealand

Introduction

THE so-called "panel" methods for calculating potential flows over lifting bodies begin with an appropriate form of Green's theorem, which requires the evaluation over the body surface of integrals involving the potential ϕ. This is done by redefining the surface as a series of panels, with ϕ taking an assumed distribution on each panel, which is sufficiently simple for the integral over the panel to be carried out analytically. The basis of the method may be found in Hunt[1] or Moran.[2] For thick airfoils and other bodies without sharp edges, the potential and its gradients are well-behaved everywhere, and the panel methods give excellent predictions of lift and induced drag. However for thin bodies, or flows that involve a sharp edge at which the Kutta condition is not satisfied, singularities appear at the sharp edges and the method becomes less well behaved. The purpose of this note is to point out that a simple modification to a conventional panel method for such problems accounts for the main effect of this singularity and produces a significant increase in accuracy.

Accounting for the Edge Singularity

Most panel methods assume a fixed value of ϕ on each of a number of surface panels, and find the local surface velocities from the local gradients of the potential. The gradients are found either numerically or by fitting a different assumed form for ϕ over the panel of interest and its neighbors. The following example is worked out for a thin two-dimensional airfoil having a sharp edge at $x = 0$. Assuming a quadratic form, the expression

$$\phi = A + Bx + Cx^2 \tag{1}$$

is fitted to the discrete values of ϕ already calculated for the nth panel and its two neighbors, using values for x at the panel control points. The velocity jump at the panel control point x_{nc} is then calculated using

$$\Delta v_n = B + 2Cx_{nc}$$

The loading is assumed constant over the element, and as it is proportional to the velocity jump the final steps are to multiply each control point velocity by the panel area A_n to give a panel force

$$f_n = A_n \Delta v_n$$

and to then sum the force components over the panels.

The primary source of inaccuracy in this process is easily demonstrated, using the known distribution for the jump in potential function near the sharp leading edge of two-dimensional airfoil

$$\phi = x^{1/2} \tag{2}$$

The airfoil surface is divided into panels of width A_n, with control points at the center of each element. Equation (2) is used to evaluate ϕ at the control points, and then the above procedure is used to find the velocity and force on the first four elements from the leading edge. The exact results for each element are also readily obtained from Eq. (2).

The results of this process are shown in Table 1 for the case of uniform panel size (unit width) when, for example, the quadratic fit of Eq. (1) to Eq. (2) over the first three elements is

$$\phi = 0.387 + 0.680x - 0.081x^2$$

It is clear from the table that the largest error by far occurs on the first panel (as expected, because the singularity is at the origin), and that on subsequent panels, the quadratic approximation gives quite good answers. The usual methods of improving the accuracy of the method are either to use higher panel density or, more properly, by moving the control points away from the panel centers in the manner described by James,[3] Guermond,[4] and others. The remedy proposed here is to account for the presence of the singularity in the leading-edge panel only, by fitting an alternative expression to the potential in that neighborhood that is derived from the exact solution for the flow around a flat plate. Specifically, Eq. (1) is replaced by

$$\phi = x^{1/2}(A + Bx) + C \tag{3}$$

for the leading-edge element, and the velocity at the control point by

$$\Delta v_1 = \frac{(A + Bx_{1c})}{\sqrt{x_{1c}}}$$

(rather than the exact expression, which would use $0.5A + 1.5Bx_{1c}$) so that when this is multiplied by the panel length, the resulting expression for the load corresponds to the correct value, as derived from Eq. (3). For the special case used as an example, this assumed form for the potential fits exactly, thus in Table 1 the estimated values of velocity and loading would be replaced by their exact values for the first element, with those for the remaining elements remaining unchanged. The estimate of total load is significantly improved as a result.

Table 1 Estimated velocity and loading near a sharp edge (uniform panels)

Element n	1	2	3	4
x_{nc}	0.5	1.5	2.5	3.5
Δv_n	0.599	0.437	0.323	0.270
Exact Δv	0.707	0.408	0.316	0.267
f_n	0.599	0.437	0.323	0.270
Exact loading	1.000	0.414	0.317	0.267

Received July 27, 1991; accepted for publication Aug. 1, 1991.

*Research Fellow, Yacht Research Unit.
†Professor, Department of Mechanical Engineering.